The Journal of Chemical Physics ARTICLE scitation.org/journal/jcp

Generalized spin mapping for quantum-classical dynamics

Cite as: J. Chem. Phys. 152, 084110 (2020); doi: 10.1063/1.5143412
Submitted: 23 December 2019 • Accepted: 9 February 2020 •
Published Online: 26 February 2020

Johan E. Runeson[a] and Jeremy O. Richardson[b]

AFFILIATIONS

Laboratory of Physical Chemistry, ETH Zürich, 8093 Zürich, Switzerland

[a]Electronic mail: johan.runeson@phys.chem.ethz.ch
[b]Author to whom correspondence should be addressed: jeremy.richardson@phys.chem.ethz.ch

ABSTRACT

We recently derived a spin-mapping approach for treating the nonadiabatic dynamics of a two-level system in a classical environment [J. E. Runeson and J. O. Richardson, J. Chem. Phys. **151**, 044119 (2019)] based on the well-known quantum equivalence between a two-level system and a spin-1/2 particle. In the present paper, we generalize this method to describe the dynamics of N-level systems. This is done via a mapping to a classical phase space that preserves the $SU(N)$-symmetry of the original quantum problem. The theory reproduces the standard Meyer–Miller–Stock–Thoss Hamiltonian without invoking an extended phase space, and we thus avoid leakage from the physical subspace. In contrast to the standard derivation of this Hamiltonian, the generalized spin mapping leads to an N-dependent value of the zero-point energy parameter that is uniquely determined by the Casimir invariant of the N-level system. Based on this mapping, we derive a simple way to approximate correlation functions in complex nonadiabatic molecular systems via classical trajectories and present benchmark calculations on the seven-state Fenna–Matthews–Olson light-harvesting complex. The results are significantly more accurate than conventional Ehrenfest dynamics, at a comparable computational cost, and can compete in accuracy with other state-of-the-art mapping approaches.

I. INTRODUCTION

The full quantum dynamics of complex systems is, in general, far too complicated to be simulated in practice. Instead, it is often necessary to separate the problem into a (small) subsystem that is treated quantum-mechanically and an environment that can be approximated by classical dynamics. In chemistry, the typical example is to treat a molecular system as a subsystem of N electronic levels coupled to an environment of classical nuclear modes. If the coupling between the electronic and nuclear motion cannot be neglected, methods based on the standard Born–Oppenheimer approximation are not applicable. Instead, new methods are needed to describe such *nonadiabatic* processes, which are important for the study of solar cells, vision, and photosynthesis, among others.[1]

One way to make large-scale simulations of these phenomena possible is to approximate the nuclear motion by an ensemble of independent trajectories that propagate under classical equations of motion. Among the simplest trajectory-based methods are Ehrenfest dynamics, in which the nuclei move on a mean-field potential defined by the instantaneous electronic populations, while the electronic variables follow exact subsystem dynamics according to the instantaneous nuclear configuration. This method has a number of known severe drawbacks[2] but is still popular due to its simplicity and low computational cost. Other options of comparable cost include surface hopping[3] and mapping-based techniques.[4] In particular, the Meyer–Miller–Stock–Thoss (MMST) mapping[5,6] has recently regained attention.[7–16] As a generalization of the Schwinger bosonization to N-level systems, its basic principle is to represent the N electronic states by N coupled harmonic oscillators that share a single excitation. This mapping is formally exact and has inspired a number of methods for calculating correlation functions, such as the linearized semiclassical initial-value representation (LSC-IVR),[17] the Poisson-bracket mapping equation (PBME),[18,19] the symmetrical quasiclassical windowing approach (SQC),[7,11] partially linearized density matrix dynamics (PLDM),[20,21] and the forward–backward trajectory solution (FBTS)[22,23] of the quantum-classical Liouville equation (QCLE).[24] These *quasiclassical* approaches all use a classical description of the nuclear dynamics

TABLE I. Formulas for the squared *XP*-radius R_s^2 and the zero-point energy parameter γ_s for general N.

s	R_s^2	γ_s
Q	2	0
W	$2\sqrt{N+1}$	$\frac{2}{N}(\sqrt{N+1}-1)$
P	$2(N+1)$	2

$$\dot{X}_n = \sum_{m=1}^{N} V_{nm} P_m, \tag{35a}$$

$$\dot{P}_n = -\sum_{m=1}^{N} V_{nm} X_m, \tag{35b}$$

$$\dot{x} = p/m, \tag{35c}$$

$$\dot{p} = -\sum_{n=1}^{N} \frac{\partial V_n}{\partial x} \frac{1}{2}(X_n^2 + P_n^2 - \gamma_s) - \sum_{n>m} \frac{\partial V_{nm}}{\partial x}(X_n X_m + P_n P_m). \tag{35d}$$

In Appendix F, we show that these equations of motion provide an approximate solution to the quantum-classical Liouville equation. We can, thus, interpret X_n and P_n defined in Eq. (28) as conjugate variables.[59]

What we have presented is a major step forward from the previously suggested spin-mapping approaches,[12,28,29] which did not recover the MMST Hamiltonian and did not reduce to the exact quantum dynamics for an isolated subsystem. One could even say that the generalized spin mapping is a more natural derivation of the MMST Hamiltonian, as it requires no extended phase space and (for s = W) directly gives a γ closer to those found optimal in numerical simulations. In the rest of this section, we will give two further reasons for this point of view.

First, the dynamics cannot take the system out of the physical phase space. Although in all MMST-mapping approaches, the length of the *XP*-radius is constant along a single trajectory, here our X_n and P_n are sampled from a hypersphere with a fixed radius of R_s (see Table I) and so the ensemble dynamics will be subtly different. Thus, in contrast to the standard MMST-mapping approaches, there can be *no leakage* out of the mapping space, thereby solving a fundamental problem of the original MMST mapping. Like in the MMST dynamics, the classical equations of motion for the X_n and P_n variables exactly correspond to the electronic Schrödinger equation for the uncoupled system.

Second, the generalized spin mapping solves an ambiguity in the definition of the potential matrix. In the literature, it is common to separate $\hat{V}(x)$ into a state-independent and a state-dependent part and the particular choice of splitting can influence the results of some methods (such as LSC-IVR and SQC). Typically authors suggested separation of the traced and traceless parts,[15,19,22] although other choices have also been used.[8,60] In our approach, the weights of the forces in Eq. (35d) always sum up to one,

$$\sum_{n=1}^{N} \tfrac{1}{2}(X_n^2 + P_n^2 - \gamma_s) = 1, \tag{36}$$

which means that it is *independent* of such a splitting. This is *not* an additional constraint but follows from the formulas for R_s^2 and γ_s in Table I.

D. Correlation functions

Now that we have specified the phase space and determined the equations of motion, we are ready to use the standard quasiclassical approximation to evaluate correlation functions of the type

$$C_{AB}(t) = \mathrm{Tr}[\hat{\rho}_\mathrm{b} \hat{A}(0) \hat{B}(t)], \tag{37}$$

where capitalized Tr means a trace over both electronic and nuclear states, $\hat{\rho}_\mathrm{b}$ is the nuclear density matrix, and the initial electronic density matrix is defined by $\hat{A}$. The trace over the electronic degrees of freedom can be written as integrals of Stratonovich–Weyl functions [see Eqs. (14) and (15)]. Likewise, the trace over the nuclei can be expressed in terms of the Wigner distribution,

$$\rho_\mathrm{b}(x,p) = \int \mathrm{e}^{\mathrm{i}py} \left\langle x - \frac{y}{2} \middle| \hat{\rho}_\mathrm{b} \middle| x + \frac{y}{2} \right\rangle \mathrm{d}y. \tag{38}$$

The correlation function can then be exactly written as

$$C_{AB}(t) = \langle A_s(X,P) [\hat{B}(t)]_{\bar{s}}(X,P) \rangle, \tag{39}$$

where $\bar{s}$ is the dual of s (that is $\bar{\mathrm{Q}}$ = P, $\bar{\mathrm{P}}$ = Q, and $\bar{\mathrm{W}}$ = W) and the expectation value is defined as

$$\langle \cdots \rangle = N \frac{\int \mathrm{d}x\, \mathrm{d}p\, \mathrm{d}X\, \mathrm{d}P \cdots \delta(X^2 + P^2 - R_s^2) \rho_\mathrm{b}(x,p)}{\int \mathrm{d}x\, \mathrm{d}p\, \mathrm{d}X\, \mathrm{d}P\, \delta(X^2 + P^2 - R_s^2) \rho_\mathrm{b}(x,p)}.$$

The factor N appears because we have multiplied and divided by $\int \mathrm{d}X\, \mathrm{d}P\, \delta(X^2 + P^2 - R_s^2) = \int \mathrm{d}\Omega = \mathrm{tr}[\hat{\mathcal{I}}] = N$. We also introduced the shorthand notation $X^2 \equiv \sum_{n=1}^{N} X_n^2$ and $P^2 \equiv \sum_{n=1}^{N} P_n^2$.

We now propose to approximate the correlation function by

$$C_{AB}(t) \approx \langle A_s(X,P) B_{\bar{s}}(X(t), P(t)) \rangle, \tag{40}$$

where the dynamics is driven by the Hamiltonian H_s in the s-representation. This formula is the multi-level generalization of the quasiclassical spin-mapping method in Ref. 27 and is used to generate the results of the full-sphere initial conditions in Sec. III. It is guaranteed to be exact for $t = 0$. One could think of the s = W case as a type of classical Wigner dynamics in *both* the nuclear and the electronic degrees of freedom.

Typically, we will be interested in population transfer from a state n to a state m, i.e., $\hat{A} = |n\rangle\langle n|$ and $\hat{B} = |m\rangle\langle m|$. The corresponding Stratonovich–Weyl functions are the population observables,

$$[|n\rangle\langle n|]_s = \tfrac{1}{2}(X_n^2 + P_n^2 - \gamma_s), \tag{41a}$$

$$[|m\rangle\langle m|]_{\bar{s}} = \tfrac{1}{2}\left(\frac{R_{\bar{s}}^2}{R_s^2}(X_m^2 + P_m^2) - \gamma_{\bar{s}}\right). \tag{41b}$$

The scaling factor $R_{\bar{s}}^2/R_s^2$ appears because the s-dependent coordinate transforms from c_n to X_n and P_n [Eq. (28)] is made globally for the entire correlation function integral, and so to get the $\bar{s}$-representation, we need to multiply by this factor. In the symmetric

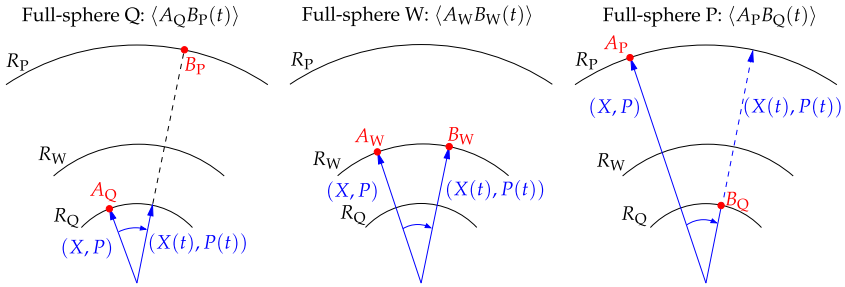

FIG. 2. Schematic picture of the full-sphere methods Q, W, and P. In the Q case, the X- and P-variables are sampled uniformly from a hypersphere with radius R_Q. The dynamics takes place entirely on this sphere, but the final-time observable is measured in variables scaled to the radius R_P. In the W case, the initial and final observables are treated on an equal footing. The P case is like Q, but reversed. All three methods are equivalent for an isolated system, but different when coupled to a nuclear environment.

case of $s = \bar{s} = \mathrm{W}$, no scaling is necessary. Figure 2 shows a schematic picture of this procedure.

It is no more difficult to calculate off-diagonal elements of the density matrix, for example,

$$[|n\rangle\langle m| + |m\rangle\langle n|]_s = X_n X_m + P_n P_m, \tag{42a}$$

$$\mathrm{i}[|n\rangle\langle m| - |m\rangle\langle n|]_s = X_n P_m - P_n X_m, \tag{42b}$$

and the $\bar{s}$-symbols are again obtained by multiplying with $R_{\bar{s}}^2/R_s^2$.

Let us now consider the impact of choosing $s \in \{\mathrm{Q}, \mathrm{P}, \mathrm{W}\}$ (again, we stress that s specifies both the Hamiltonian H_s and the initial distribution through R_s). The alternatives are to calculate the correlation function in a symmetric way, meaning $(s, \bar{s})$=(W, W), or in an asymmetric way, that is, $(s, \bar{s})$=(Q, P) or (P, Q). In Ref. 27, we saw that (Q, P) and (W, W) both gave accurate results for a wide range of spin–boson models, while (P, Q) was always less accurate. After running tests on further systems, we have observed that (Q, P) is not always so reliable but that the symmetric definition (W, W) is the most robust. This is confirmed by the results we show in Sec. III and in the supplementary material. In Appendix F, we show that the dynamics is valid to one higher order in $\hbar$ when using $s = \mathrm{W}$ than with other choices of s.

In practice, we employ the following procedure to evaluate Eq. (40): first, we sample x, p from the Wigner distribution $\rho_\mathrm{b}(x, p)$ and X, P uniformly from the sphere $X^2 + P^2 = R_s^2$. The latter is easy to implement by drawing X, P from a standard normal distribution and rescaling them with a common factor $R_s/\sqrt{X^2 + P^2}$. Then, we propagate these variables with the equations of motion (35) using a modified velocity Verlet scheme.[61] Finally, we average over the trajectories until convergence. Note that this gives the results of all $n \to m$ transitions in a single simulation. We will refer to the sampling from $\delta(X^2 + P^2 - R_s^2)$ as *full-sphere* initial conditions. This type of initial condition has also been considered by He and Liu,[13] but within our notation, their approach (CMM2) would be described as (Q, Q), i.e., they used the Q-representation at both initial and final times, in contrast to what we derived from the Stratonovich–Weyl theory. (However, for two-level spin–boson models, the results appear to be of similar quality.)[13,27]

In essence, the approach is to sample points on a hypersphere, propagate them, measure observables from the new directions, and average. The evolution of the angles is simple to express in terms of the $2N$ Cartesian coordinates X_n and P_n, and their magnitude R_s takes care of the different weighting of trace-containing and traceless parts of the Hamiltonian and the observables. Since R_s is constant and (as a consequence) the dynamics is invariant to a cyclic coordinate,[59] the number of relevant degrees of freedom is $2N - 2$, just like in the original quantum problem.

E. Focused initial conditions

Previous authors in the mapping community have also used an approximation called *focused* initial conditions.[5,18,23,25–27,62–64] This approach does not rely on SW-representations, but we consider it here to facilitate comparison with previous work. In the case of $\hat{A} = |n\rangle\langle n|$, the focused initial distribution only includes points that have $A_s(X, P) = 1$, rather than by weighting as in Eq. (40). This means that $\frac{1}{2}(X_n^2 + P_n^2 - \gamma_s) = 1$, while $\frac{1}{2}(X_k^2 + P_k^2 - \gamma_s) = 0$ for all $k \neq n$, or equivalently

$$X_k = r_k \cos\phi_k, \quad P_k = r_k \sin\phi_k, \tag{43}$$

with $r_{k=n} = \sqrt{2 + \gamma_s}$, $r_{k\neq n} = \sqrt{\gamma_s}$ and uniformly sampled $\phi_k \in [0, 2\pi)$. One can interpret this as sampling from the "polar circles" in Fig. 1. In the correlation function, $A_s(X, P) = 1$ by construction so that we define the focused spin-mapping method as

$$C_{AB}(t) \approx \langle B_s(X(t), P(t))\rangle_\mathrm{foc}, \tag{44}$$

where

$$\langle\cdots\rangle_\mathrm{foc} = \frac{\int \mathrm{d}x\,\mathrm{d}p\,\mathrm{d}X\,\mathrm{d}P \cdots \rho_\mathrm{foc}(X, P)\rho_\mathrm{b}(x, p)}{\int \mathrm{d}x\,\mathrm{d}p\,\mathrm{d}X\,\mathrm{d}P\,\rho_\mathrm{foc}(X, P)\rho_\mathrm{b}(x, p)}$$

uses the focused distribution

$$\rho_\mathrm{foc}(X, P) = \delta(X_n^2 + P_n^2 - \gamma_s - 2)\prod_{k\neq n}\delta(X_k^2 + P_k^2 - \gamma_s) \tag{45}$$

and trajectories are defined according to H_s. Note that for focused methods, the observable $B_s(X(t), P(t))$ must be calculated with the *same* index s as the Hamiltonian, in contrast to methods that use full-sphere initial conditions.[65] One advantage of using focused initial conditions is that Eq. (44) typically requires an order of magnitude fewer trajectories to converge compared to Eq. (40), and we shall see in Sec. III that they give practically identical results for $s = \mathrm{W}$. It is possible to define focused initial conditions also when starting from off-diagonal elements of the density matrix, as explained in Ref. 27.